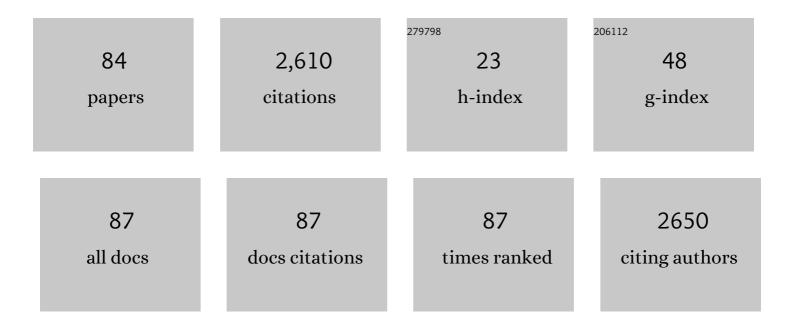
List of Publications by Year in descending order

Source: https://exaly.com/author-pdf/4227362/publications.pdf Version: 2024-02-01



#	Article	IF	CITATIONS
1	Effect of Multiple Repair Welding on Crack Susceptibility and Mechanical Properties of Inconel 718 Alloy Casting. Journal of Materials Engineering and Performance, 2022, 31, 254-261.	2.5	5
2	Interfacial characteristics of P91 steel - Inconel 740H bimetallic structure fabricated using wire-arc additive manufacturing. Journal of Materials Processing Technology, 2022, 300, 117396.	6.3	15
3	Phase transformations and mechanical behavior in a non-equiatomic Ti10Fe30Co30Ni30 medium-entropy alloy. Materials Science & Engineering A: Structural Materials: Properties, Microstructure and Processing, 2022, 832, 142429.	5.6	8
4	Introducing Heusler intermetallics for synergic effect of grain refinement and precipitation strengthening in high-strength low-alloy steels. Journal of Alloys and Compounds, 2022, 904, 163885.	5.5	4
5	Phase transformations during continuous cooling in Inconel 718 alloys manufactured by laser powder bed fusion and suction casting. Materials Characterization, 2022, 185, 111764.	4.4	7
6	Functionally Graded Alloys from 316 Stainless Steel to Inconel 718 by Powder-Based Laser Direct Energy Deposition. Minerals, Metals and Materials Series, 2022, , 304-312.	0.4	1
7	Target-Sintering of Single-Phase Bulk Intermetallics via a Fast-Heating-Induced Rapid Interdiffusion Mechanism. , 2022, 4, 480-486.		6
8	Determination of Location-Specific Solidification Cracking Susceptibility for a Mixed Dissimilar Alloy Processed by Wire-Arc Additive Manufacturing. Metals, 2022, 12, 284.	2.3	3
9	Effects of Magnetic Abrasive Finishing on Microstructure and Mechanical Properties of Inconel 718 Processed by Laser Powder Bed Fusion. Journal of Manufacturing and Materials Processing, 2022, 6, 43.	2.2	2
10	Thermal Conductivity Determination of Ga-In Alloys for Thermal Interface Materials Design. Thermo, 2022, 2, 1-13.	1.3	2
11	Wire-arc additive manufacturing and post-heat treatment optimization on microstructure and mechanical properties of Grade 91 steel. Additive Manufacturing, 2021, 37, 101734.	3.0	12
12	Phase Transformations During Homogenization of Inconel 718 Alloy Fabricated by Suction Casting and Laser Powder Bed Fusion: A CALPHAD Case Study Evaluating Different Homogenization Models. Journal of Phase Equilibria and Diffusion, 2021, 42, 28-41.	1.4	7
13	Rapid Synthesis and Sintering of Metals from Powders. Advanced Science, 2021, 8, e2004229.	11.2	23
14	Integration of Processing and Microstructure Models for Non-Equilibrium Solidification in Additive Manufacturing. Metals, 2021, 11, 570.	2.3	15
15	Influence of long-term aging on microstructural stability and performance of DD6 superalloy. Materials Science and Technology, 2021, 37, 607-615.	1.6	1
16	Phase Stability and Microhardness of the AlxCr2-xCoFeNi High-Entropy Alloys. Journal of Phase Equilibria and Diffusion, 2021, 42, 379-388.	1.4	3
17	CALPHAD modeling based on Gibbs energy functions from zero kevin and improved magnetic model: A case study on the Cr–Ni system. Calphad: Computer Coupling of Phase Diagrams and Thermochemistry, 2021, 73, 102268.	1.6	11
18	Impact of homogenization on microstructure-property relationships of Inconel 718 alloy prepared by laser powder bed fusion. Materials Science & Engineering A: Structural Materials: Properties, Microstructure and Processing, 2021, 826, 141973.	5.6	15

#	Article	IF	CITATIONS
19	An evaluation of the Mn–Ga system: Phase diagram, crystal structure, magnetism, and thermodynamic properties. Calphad: Computer Coupling of Phase Diagrams and Thermochemistry, 2020, 68, 101722.	1.6	12
20	A Discrete Dendrite Dynamics Model for Epitaxial Columnar Grain Growth in Metal Additive Manufacturing with Application to Inconel. Additive Manufacturing, 2020, 36, 101611.	3.0	14
21	A new high-throughput method using additive manufacturing for alloy design and heat treatment optimization. Materialia, 2020, 13, 100835.	2.7	14
22	Thermodynamic Investigation of New High-Strength Low-Alloy Steels with Heusler Phase Strengthening for Welding and Additive Manufacturing: High-Throughput CALPHAD Calculations and Key Experiments for Database Verification. Journal of Phase Equilibria and Diffusion, 2020, 41, 804-818.	1.4	12
23	Enhanced Resistance to Irradiation Induced Ferritic Transformation in Nanostructured Austenitic Steels. Materialia, 2020, 13, 100806.	2.7	9
24	Stacking fault energy prediction for austenitic steels: thermodynamic modeling vs. machine learning. Science and Technology of Advanced Materials, 2020, 21, 626-634.	6.1	18
25	Uncertainty quantification and composition optimization for alloy additive manufacturing through a CALPHAD-based ICME framework. Npj Computational Materials, 2020, 6, .	8.7	20
26	Effect of solution treatment on micropore and mechanical properties of DD6 superalloy. Materials Science and Technology, 2020, 36, 1980-1987.	1.6	1
27	Post-heat treatment design for high-strength low-alloy steels processed by laser powder bed fusion. Materials Science & Engineering A: Structural Materials: Properties, Microstructure and Processing, 2020, 788, 139531.	5.6	14
28	Cyclic re-austenitization of copper-bearing high-strength low-alloy steels fabricated by laser powder bed fusion. Materials Characterization, 2020, 166, 110437.	4.4	10
29	A comparative analysis of Inconel 718 made by additive manufacturing and suction casting: Microstructure evolution in homogenization. Additive Manufacturing, 2020, 36, 101404.	3.0	15
30	A new thermodynamic modeling of the Ti–V system including the metastable ω phase. Intermetallics, 2020, 122, 106791.	3.9	18
31	Influence of synthesis method on microstructure and mechanical behavior of Co-free AlCrFeNi medium-entropy alloy. Intermetallics, 2019, 108, 45-54.	3.9	48
32	Martensite Start Temperature Predictor for Steels Using Ensemble Data Mining. , 2019, , .		4
33	A high-entropy alloy with hierarchical nanoprecipitates and ultrahigh strength. Science Advances, 2018, 4, eaat8712.	10.3	247
34	Quantitative Texture Prediction of Epitaxial Columnar Grains in Alloy 718 Processed by Additive Manufacturing. Minerals, Metals and Materials Series, 2018, , 749-755.	0.4	1
35	Investigation on Phase Stability of AlxCo0.2Cr0.2Ni0.2Ti0.4 â^ x High Entropy Alloys. Journal of Phase Equilibria and Diffusion, 2018, 39, 610-622.	1.4	9
36	Characterization of nano-scale oxides in austenitic stainless steel processed by powder bed fusion. Scripta Materialia, 2018, 155, 104-108.	5.2	220

#	Article	IF	CITATIONS
37	Simulation-aided constitutive law development – Assessment of low triaxiality void nucleation models via extended finite element method. Journal of the Mechanics and Physics of Solids, 2017, 102, 30-45.	4.8	9
38	Mean-field polycrystal plasticity modeling with grain size and shape effects for laser additive manufactured FCC metals. International Journal of Solids and Structures, 2017, 112, 35-42.	2.7	29
39	Thermodynamic re-assessment of the Al-Co-W system. Calphad: Computer Coupling of Phase Diagrams and Thermochemistry, 2017, 59, 112-130.	1.6	52
40	Effect of solution treatment on spinodal decomposition during aging of an Fe-46.5 at.% Cr alloy. Journal of Materials Science, 2017, 52, 326-335.	3.7	17
41	Grain Structure Control of Additively Manufactured Metallic Materials. Materials, 2017, 10, 1260.	2.9	223
42	Cybermaterials: materials by design and accelerated insertion of materials. Npj Computational Materials, 2016, 2, .	8.7	53
43	Linking process, structure, property, and performance for metal-based additive manufacturing: computational approaches with experimental support. Computational Mechanics, 2016, 57, 583-610.	4.0	190
44	Thermodynamically consistent microstructure prediction of additively manufactured materials. Computational Mechanics, 2016, 57, 359-370.	4.0	54
45	Integrated computational materials design for high-performance alloys. MRS Bulletin, 2015, 40, 1035-1044.	3.5	50
46	CALPHAD-Based Integrated Computational Materials Engineering Research for Materials Genomic Design. Jom, 2015, 67, 1864-1865.	1.9	5
47	Direct atom probe tomography observations of concentration fluctuations in Fe–Cr solid solution. Scripta Materialia, 2015, 98, 13-15.	5.2	17
48	Thermodynamic models of low-temperature Mn-Ni-Si precipitation in reactor pressure vessel steels. MRS Communications, 2014, 4, 101-105.	1.8	31
49	Thermodynamic modelling of crystalline unary phases. Physica Status Solidi (B): Basic Research, 2014, 251, 14-32.	1.5	55
50	Thermodynamic evaluation of the Np–Zr system using CALPHAD and ab initio methods. Journal of Nuclear Materials, 2014, 452, 569-577.	2.7	9
51	Thermodynamic modeling of the U–Zr system – A revisit. Journal of Nuclear Materials, 2013, 443, 331-341.	2.7	60
52	Correlation and relativistic effects in U metal and U-Zr alloy: Validation of <i>ab initio</i> approaches. Physical Review B, 2013, 88, .	3.2	74
53	An improved magnetic model for thermodynamic modeling. Calphad: Computer Coupling of Phase Diagrams and Thermochemistry, 2012, 39, 11-20.	1.6	53
54	A new approach to establish both stable and metastable phase equilibria for fcc ordered/disordered phase transition: application to the Al–Ni and Ni–Si systems. Materials Chemistry and Physics, 2012, 135, 94-105.	4.0	23

#	Article	IF	CITATIONS
55	3D Analysis of Phase Separation in Ferritic Stainless Steels. , 2012, , 221-226.		2
56	Thermodynamic investigation of the galvanizing systems, II: Thermodynamic evaluation of the Ni–Zn system. Calphad: Computer Coupling of Phase Diagrams and Thermochemistry, 2011, 35, 276-283.	1.6	17
57	An improved thermodynamic modeling of the Fe–Cr system down to zero kelvin coupled with key experiments. Calphad: Computer Coupling of Phase Diagrams and Thermochemistry, 2011, 35, 355-366.	1.6	141
58	Magnetic phase diagram of the Fe–Ni system. Acta Materialia, 2011, 59, 521-530.	7.9	73
59	Thermodynamic modeling of the Feâ Zn system using exponential temperature dependence for the excess Gibbs energy. Journal of Mining and Metallurgy, Section B: Metallurgy, 2011, 47, 1-10.	0.8	13
60	Phase Equilibria and Thermodynamic Properties in the Fe-Cr System. Critical Reviews in Solid State and Materials Sciences, 2010, 35, 125-152.	12.3	172
61	Elastic and thermodynamic properties of the Ni–B system studied by first-principles calculations and experimental measurements. Calphad: Computer Coupling of Phase Diagrams and Thermochemistry, 2010, 34, 245-251.	1.6	15
62	Carbon – Tungsten – Zirconium. Landolt-Bâ^šâ^,rnstein - Group IV Physical Chemistry, 2010, , 31-47.	0.0	4
63	Experimental investigation and thermodynamic modeling of the ternary Al–Cu–Fe system. Journal of Materials Research, 2009, 24, 3154-3164.	2.6	45
64	Thermodynamic Assessment of the Cu-B System Supported by Key Experiment and First-Principles Calculations. Journal of Phase Equilibria and Diffusion, 2009, 30, 480-486.	1.4	7
65	Iron – Silicon – Zirconium. Landolt-Bâ^šâ^,rnstein - Group IV Physical Chemistry, 2009, , 605-620.	0.0	3
66	Thermodynamic investigation of the galvanizing systems, I: Refinement of the thermodynamic description for the Fe–Zn system. Calphad: Computer Coupling of Phase Diagrams and Thermochemistry, 2009, 33, 433-440.	1.6	44
67	Phase equilibria of the Fe–Ni–Si system at 850°C. Journal of Alloys and Compounds, 2009, 481, 509-514.	5.5	16
68	Reassessment of the Ni–B system supported by key experiments and first-principles calculation. International Journal of Materials Research, 2009, 100, 59-67.	0.3	9
69	Iron – Silicon – Titanium. Landolt-Bâ^šâ^,rnstein - Group IV Physical Chemistry, 2009, , 555-578.	0.0	0
70	Reaction Scheme and Liquidus Surface in the Al-Rich Section of the Al-Cr-Ni System. Metallurgical and Materials Transactions A: Physical Metallurgy and Materials Science, 2008, 39, 2363-2369.	2.2	13
71	Experimental investigation of the Al–Ce–Ni system at 800°C. Intermetallics, 2008, 16, 432-439.	3.9	16
72	Thermodynamic modeling of the V–Si system supported by key experiments. Calphad: Computer Coupling of Phase Diagrams and Thermochemistry, 2008, 32, 320-325.	1.6	40

0

#	Article	IF	CITATIONS
73	Thermodynamic reassessment of the Cu–Mg–Ni system with brief comments on the thermodynamic modeling of the sub-systems. Calphad: Computer Coupling of Phase Diagrams and Thermochemistry, 2008, 32, 675-685.	1.6	11
74	Construction of the Al–Ni–Si phase diagram over the whole composition and temperature ranges: thermodynamic modeling supported by key experiments and first-principles calculations. International Journal of Materials Research, 2008, 99, 598-612.	0.3	21
75	Phase equilibria of the Al–Ni–Zn system at 340°C. International Journal of Materials Research, 2008, 99, 644-649.	0.3	11
76	Reassessment of the Ce–Ni binary system supported by key experiments and ab initio calculations. Intermetallics, 2007, 15, 1401-1408.	3.9	24
77	Experimental study of the Be–Si phase diagram. Journal of Materials Science, 2006, 41, 2525-2528.	3.7	11
78	N-Ti-V (Nitrogen - Titanium - Vanadium). Landolt-Bâ^šâ^,rnstein - Group IV Physical Chemistry, 2006, , 1-10.	0.0	0
79	Thermodynamic assessment of the Mo–Nb–Ta system. Calphad: Computer Coupling of Phase Diagrams and Thermochemistry, 2004, 28, 133-140.	1.6	56
80	Ce-Ru-Si (Cerium - Ruthenium - Silicon). , 0, , 1-9.		0
81	Investigation of Spinodal Decomposition in Fe-Cr Alloys: CALPHAD Modeling and Phase Field Simulation. Solid State Phenomena, 0, 172-174, 1060-1065.	0.3	14
82	3D Analysis of Phase Separation in Ferritic Stainless Steels. , 0, , 221-226.		0
83	Cu-Ga-Pd (Copper - Gallium - Palladium). , 0, , 1-12.		0

84 Cu-Pd-Pt (Copper - Palladium - Platinum). , 0, , 1-8.

6